Transient Performance Improvement of Micro-grid by a Resistive Superconducting Fault Current Limiter

Feng Zheng, Changhong Deng, Lei Chen, *Member, IEEE*, Shichun Li, Yang Liu, and Yuxiang Liao

Abstract—In this paper, a resistive type superconducting fault current limiter (SFCL) is suggested to improve the transient performance of a micro-grid system during a fault. The micro-grid is connected to the main network at the point of common coupling (PCC), where the resistive type SFCL is applied. When a short-circuit fault happens at the connecting line, the SFCL can mitigate the fault current, and its action signal will be sent to the master distributed generation (DG) included in the micro-grid. Accordingly, the switching between the master DG's two control patterns can be flexibly performed, and further the micro-grid system is expected to achieve a smooth transition between its grid-connected and islanded modes. Theoretical analysis as well as technical discussion is conducted, and the simulation model of a typical micro-grid with the SFCL is built in MATLAB. From the demonstrated results, employing the resistive type SFCL can effectively limit the transient fault current to a lower level, and meantime help to guarantee the micro-grid system's power balance and enhance its voltage and frequency stability.

Index Terms—Distributed generation, micro-grid, resistive superconducting fault current limiter, transient performance.

I. INTRODUCTION

IN RECENT years, resistive type superconducting fault current limiters (SFCLs) have attracted more attention around the world [1]-[3], and their applications in existing and future electrical distribution systems can theoretically solve some kinds of technical issues. In a sense, current-limiting devices are becoming increasingly important because of the connection of distributed generation (DG), whose access capacity can result in a higher fault-current level.

A micro-grid system can be designed to accommodate high penetration of DG units and improve the energy efficiency, and it is crucial to ensure the micro-grid system's power quality and service reliability during a fault. Typically, a micro-grid system has two modes of operation, called as grid-connected and islanded. When a short-circuit fault occurs in the main network, the micro-grid may be tripped off.
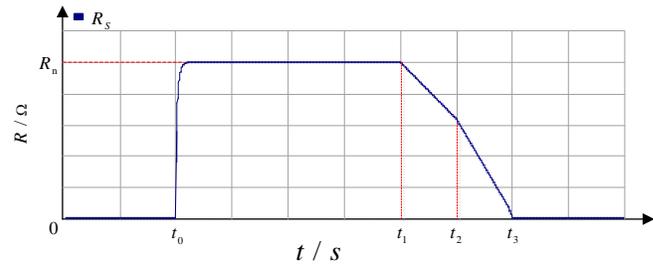
Fig. 1. Quenching and recovery characteristics of a resistance type SFCL.

According to [4]-[6], reasonably controlling the master DG is a basic method of guaranteeing the micro-grid's transient behaviors under the islanded condition. Nevertheless, in the case that the resistive type SFCL's rapid quenching characteristic and its potential effects on inhibiting current rush are taken into account, the micro-grid may achieve a more smooth transition and stable operation.

In this paper, the application of a resistive type SFCL in a typical micro-grid system is assessed. The article is organized in the following manner. Section II presents the SFCL's working principle as well as influence mechanism to the micro-grid's transient performance, and also discusses some technical issues about the device design. In section III, the model of the micro-grid integrated with the SFCL is built in MATLAB/SIMULINK, and the simulation analysis on different cases is conducted. In section IV, conclusions are summarized and next steps are suggested.

II. THEORETICAL ANALYSIS

A. Modeling of the Resistive SFCL

Based on the experimental studies for a resistive SFCL being applied in the actual power distribution system [7], its mathematical model can be expressed as:

$$R(t) = \begin{cases} 0 & (t < t_0) \\ R_n[1-\exp(-\frac{t-t_0}{\tau})]^{1/2} & (t_0 \leq t < t_1) \\ a_1(t-t_1)+b_1 & (t_1 \leq t < t_2) \\ a_2(t-t_2)+b_2 & (t_2 \leq t < t_3) \\ 0 & (t \geq t_3) \end{cases} \tag{1}$$

Where R_n and τ represent the impedance being saturated at normal temperature and time constant, respectively. In addition, t_0, t_1, and t_2 represent quench-starting time, the first recovery-starting time, and the secondary recovery-starting time, respectively. In the case of properly adjusting the
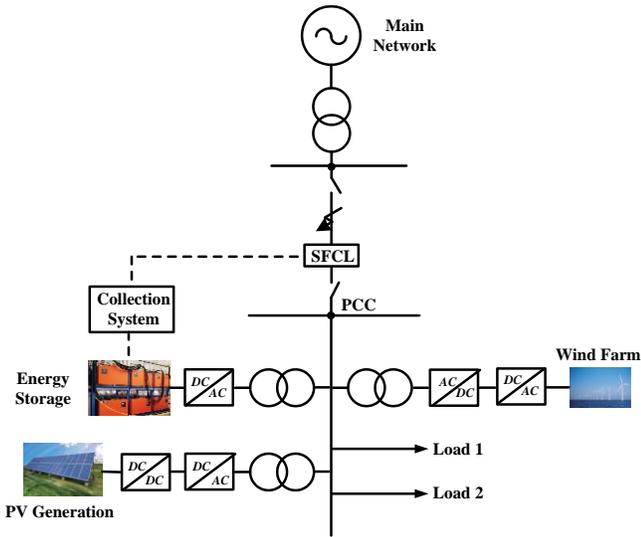
Fig. 2. Schematic diagram of a typical micro-grid integrated with the SFCL.

thermal environment and setting the system parameters, the SFCL's recovery time may be less than 0.5 s [8], so as to match up the auto-reclosing's operation. As shown in Fig. 1, it indicates the detailed quenching and recovery characteristics.

B. Influence of the Resistive SFCL on a Micro-grid's Transient Performance

The schematic diagram of a typical micro-grid integrated with the resistive SFCL is shown in Fig. 2, where the SFCL is installed at the point of common coupling (PCC) between the micro-grid and the main network. In regards to the energy storage device, photovoltaic (PV) plant and wind farm, all of these DG units are accessed to the micro-grid through the inverters [9], [10]. Note that, the energy storage device will be served as a master DG, which is used for stabilizing the micro-grid. In general, the maser DG has two control patterns, so called as the P-Q control and the V-f control.

When the micro-grid is under the grid-connected state, each of the DG units will use the P-Q control. In the case that a short-circuit fault happens in the main network, the micro-grid may be operated to work in the islanded state. The master DG's objective is to maintain the micro-grid's frequency and voltage stability as far as possible, and its control pattern will switch to the V-f control from the original P-Q control. As reasonably controlling the master DG is a basic method of ensuring the transient performance, employing the resistive type SFCL is expected to affect the control mechanism more actively and make the transition process be more smooth. Due to the SFCL's rapid quenching characteristics, it can be conducted as a control trigger since the fault current is timely detected to be larger than its critical value. That is to say, the SFCL's trigger signal caused by the superconducting-normal (S-N) transition will be sent to a collection system, and then be used for activating the master DG's control switching.

Concerning how to effectively implement the master DG's control switching, a feasible way is presented as follows. Fig. 3 shows the control strategy of the energy storage device in consideration of the resistive SFCL's trigger signal, From this
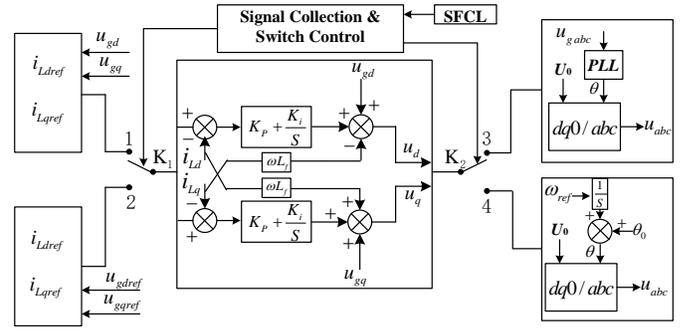

Fig. 3. Control strategy of the energy storage device in consideration of the resistive SFCL's trigger signal.

figure, specialized current-input and voltage-output channels are arranged for controlling the master DG. The channels 1 and 3 are used for realizing the master DG's P-Q control [11], [12], and the current-input references (i_{Ldref}, i_{Lqref}) can be expressed as:

$$\begin{cases} i_{Ldref} = \dfrac{2}{3}\dfrac{P_{gref}u_{gd}+Q_{gref}u_{gq}}{u^2_{gd}+u^2_{gq}} \\[3mm] i_{Lqref} = \dfrac{2}{3}\dfrac{P_{gref}u_{gq}-Q_{gref}u_{gd}}{u^2_{gd}+u^2_{gq}} \end{cases} \quad (2)$$

Where P_{gref} and Q_{gref} are the given power references; u_{gd} and u_{gq} are respectively the d-axis and q-axis components of the network-side voltage.

According to the control block diagram as demonstrated in Fig. 3, the P-Q control's output-voltage signals (u_d, u_q) can be obtained. From the figure, the following variables are defined. ω is the fundamental angular frequency; L_f is the filter inductance; i_{Ld} and i_{Lq} are the d-axis and q-axis components of the energy storage converter's output current.

On the other side, the channels 2 and 4 are used to achieve the master DG's V-f control. Based on the given network-side voltage references (u_{gdref}, u_{gqref}), the V-f control's current-input references (i_{Ldref}, i_{Lqref}) can be expressed as:

$$\begin{cases} i_{Ldref} = (K_{P1}+\dfrac{K_{i1}}{s})(u_{gdref}-u_{gd})-\omega C_f u_{gq}+i_{gd} \\[3mm] i_{Lqref} = (K_{P1}+\dfrac{K_{i1}}{s})(u_{gqref}-u_{gq})+\omega C_f u_{gd}+i_{gq} \end{cases} \quad (3)$$

Where C_f is the filter capacitance; K_{p1}, K_{i1} are the proportional and integral parameters of the voltage regulator; i_{gd} and i_{gq} are the d-axis and q-axis components of the network-side current. In a similar way, the V-f control's output-voltages (u_d, u_q) can be obtained.

In accordance to the resistive SFCL's quenching trigger, using the logical switches K_1 and K_2 can precisely implement the control switching for the master DG. It should be pointed out that, the resistive SFCL also has the responsibility of limiting the fault current from the micro-grid to the short-circuit location. Before the static-state switch equipped at the PCC is operated to make the micro-grid be disconnected from the main network, the current fluctuations can be suppressed within an acceptable level, and thus the micro-grid's transient behaviors can be ensured more effectively.

C. Technical Discussion on the Design of the SFCL

• **Superconducting material.** Currently, the bulk Bi series and $YBa_2Cu_3O_x$(YBCO) second-generation (2G) are the main high temperature superconducting (HTS) materials for electric power applications [13], [14]. Considering that the commercial YBCO 2G tapes may have the high resistivity matrix with a linear resistance of 0.354 Ω/m, the transition to the normal-conducting state may occur from 2 ms up to 4 ms after the start of fault current. Besides, the YBCO 2G tapes with stainless steel reinforcement can provide good mechanical properties, such as tensile strength above 250 MPa at room temperature. Since the YBCO 2G components may actuate faster than the Bi-2212 components [15], [16], and the expected current-limitation is higher for the YBCO 2G components after the S-N transition, the YBCO 2G tapes may be more suitable for making the resistive SFCL.

• **AC loss.** In a sense, the AC loss will be an important factor affecting the SFCL's engineering application. Its AC loss can be measured with a standard electrical technique, and also be calculated by finite-element simulations. Theoretically, the superconductor's electrical properties may be modeled with a nonlinear power law where voltage varies as $(J/J_c)^n$. J and J_c are respectively the current and critical current density. The critical current density J_c and the power index n can be derived from the measured DC current-voltage characteristics. Accordingly, the AC loss can be computed in:

$$P = f \int_0^{1/f} \int_S \mathbf{J} \cdot \mathbf{E} \, dSdt \qquad \text{(W/ m)} \qquad (4)$$

Where f is the frequency, S is the superconductor's cross-section, and $\mathbf{J}$ and $\mathbf{E}$ are the current density and the electric field at each example finite element method (FEM) node. From the simulation and experimental results in [17], the AC loss will be reduced in the presence of externally applied AC magnetic field, but be increased in the presence of AC transport current. To reduce the SFCL's AC loss as much as possible, the coupling transformer with the superconducting limiting coil may be properly considered.

• **Electrical Insulation.** In the case of that the sub-cooled liquid nitrogen is used to be the SFCL's cooling system, the dielectric strength and bubble suppression effect as the electrical insulation design's factors in the cryostat can be enhanced by increased pressure. Through injecting the non-condensable gas such as gaseous helium (GHe) or gaseous-neon (GNe) into the cryostat, the pressure of the cooling system can be controlled [18]. In addition, the gap distance between a cryostat and superconducting tapes is one of the emphasis factors of the SFCL's insulation design. According to [19], the shield ring attached to the copper current lead can reduce the gap distance between the cryostat and the SFCL. And based on the request of AC withstand voltage and shield ring's diameter, the gap distance can be designed.

From the aforementioned brief discussions, some preliminary conclusions can be obtained, and the detailed engineering design of the SFCL for an actual micro-grid system will be performed in the near future.
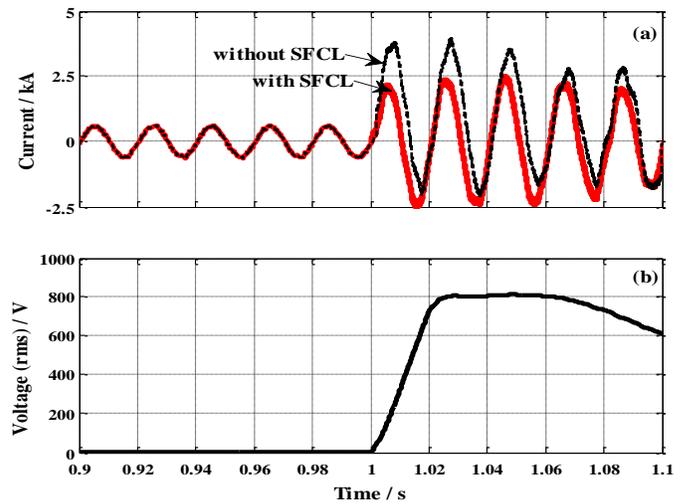

Fig. 4. Operating characteristics of the suggested resistive type SFCL. (a) fault current at the PCC and (b) RMS voltage across the SFCL's two terminals.

TABLE I
MAIN SIMULATION PARAMETERS OF THE SYSTEM MODEL

Micro-grid System	
Energy Storage	(800 V / 1000 Ah) $\times$5
PV Plant	100 kW $\times$10
Wind Farm	260 kW $\times$ 10
Load 1	0.2 MW
Load 2	0.1 MW+j0.05 Mvar
Voltage/Frequency	3 kV / 50 Hz
Resistive type SFCL	
Normal-state Resistance	1 Ω

III. SIMULATION STUDY

To quantitatively evaluate the resistive type SFCL's effects on a micro-grid system's transient performance, the simulation model corresponding to Fig. 2 is built in MATLAB/ SIMULINK, and parts of simulation parameters are indicated as Table I.

The access voltage of the demonstrated micro-grid system is selected as 3 kV, and the short-circuit fault is supposed to happen at the middle of the connecting line. During the simulation analysis, it is set that the fault occurs at $t_0 = 1$ s and lasts for 100 ms. Further, the static-state switch will be operated at t=1.1 s, and the micro-grid system will carry out the transition from its grid-connected mode to islanded mode. Herein two different simulation cases are considered and respectively reordered as case I and case II. For the former, the SFCL is not applied, and the control switching will be implemented after the fault is cleared. Regarding the latter, the resistive SFCL is employed, and this suggested device will be used for current-limitation and control trigger.

Before the fault happens, the micro-grid is connected to the main network, and a certain power exchange between them is generated. There are about 1.8 MW active power and 0.05 Mvar reactive power exporting to the main network. That is to
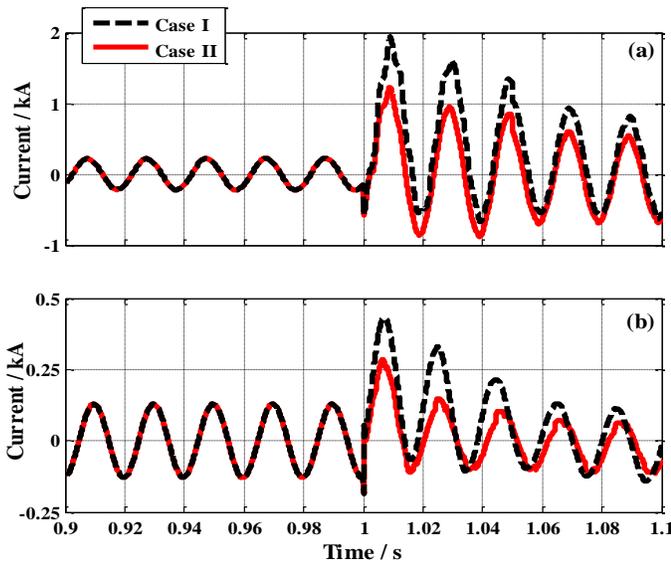
Fig. 5. Waveforms of the fault current provided by the DG included in the micro-grid with and without the SFCL. (a) wind farm and (b) PV plant.

TABLE II
FIRST PEAK OF THE FAULT CURRENT AT DIFFERENT LOCATIONS

Measuring point	Without SFCL	With the SFCL	Current-limiting ratio
PCC	3.8 kA	2.1 kA	44.7%
Wind farm	1.9 kA	1.1 kA	42.1%
PV plant	0.4 kA	0.255 kA	36.2%

say, the DG units included in the micro-grid can not only meet the two local loads' power requirements, but also provide the energy to the accessed main network. After the fault, the resistive SFCL will play its role in time. Fig. 4 shows the operating characteristics of the resistive type SFCL. Owing to the increased fault current, the maximum value (root-mean-square, RMS value) of the SFCL's terminal-voltage can be up to 800 V. In consideration of that the fault current will be quickly detected to be larger than the critical value, it is assumed that once the terminal-voltage is detected to be larger than 200V and can last for 5 ms (a quarter of power-frequency cycle), the master DG's control transition will be activated.

Fig. 5 shows the characteristics of the fault currents provided by the wind farm and the PV plant, and the SFCL's effects are also taken into account. Table II expresses the detailed data results. In terms of Fig. 4 and Fig. 5, the resistive SFCL's current-limiting characteristics can be verified, and the decrease of the overcurrent inrush will have a positive influence on the micro-grid.

Figs. 6-7 denote the bus-voltage, exchange power and frequency characteristics of the micro-grid during the control switching. It can be observed that, the application of the resistive SFCL can bring comprehensive contributions to improve the micro-grid's performance. Applying the SFCL can make the micro-grid's PCC voltage be maintained at 0.5 pu, compared to that the PCC voltage will down to 0.08 pu without SFCL, and the expected increasing rate is approximate to 84%. In addition, employing the resistive SFCL can make
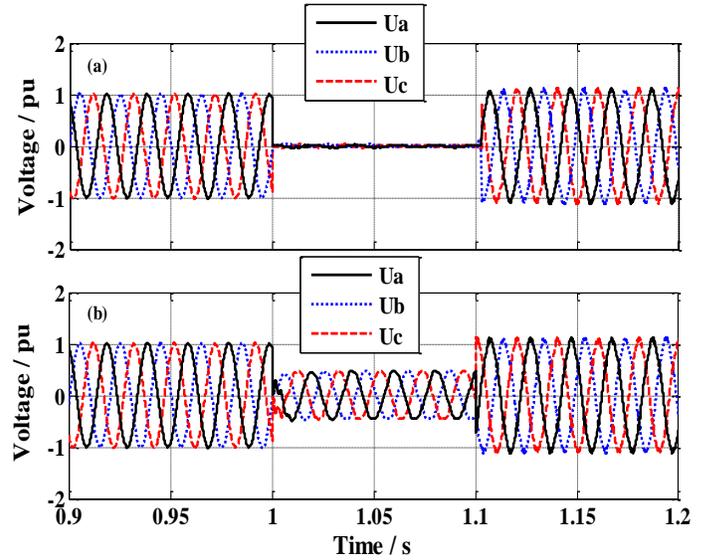

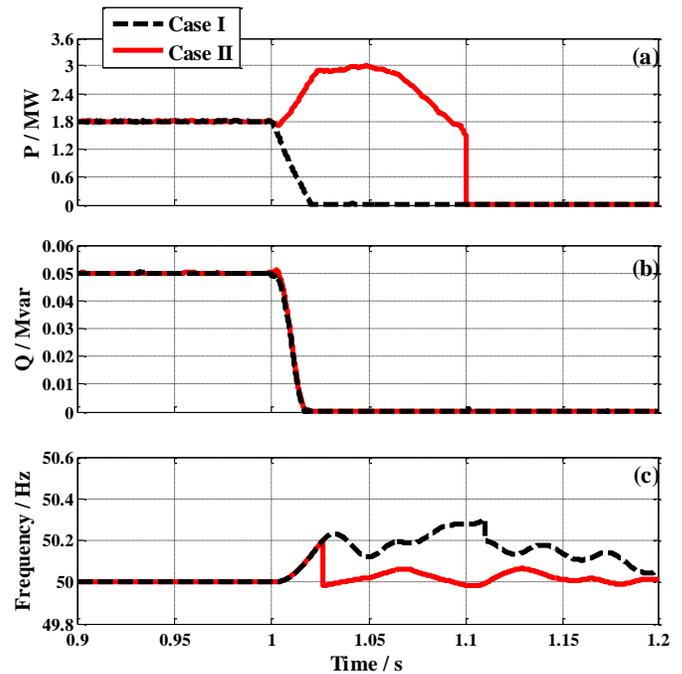Fig. 6. Waveforms of the micro-grid's PCC voltage during the fault. (a) case I and (b) case II.

Fig. 7. Transient characteristics of the micro-grid system during the fault. (a) active power exchange, (b) reactive power exchange and (c) system frequency.

the micro-grid achieve a smooth transition, where the reliability of power supply can be increased to a certain extent, and the SFCL's current-limiting resistance can effectively absorb the surplus power, so as to restrain the frequency variations. Because of that the micro-grid's power quality is a critical assessment index, the SFCL's impacts on the system frequency is analyzed. The frequency's maximum deviation is about 0.3 Hz without SFCL, and when the SFCL plays its role, the frequency's fluctuating margin will be smaller than 0.1 Hz. As a result, the enhancement of the frequency quality will be helpful to stabilize the power sources and local loads.

IV. CONCLUSION

In this paper, concerning the transient performance enhancement of a micro-grid system during a fault, a resistive type superconducting fault current limiter is suggested to play the role. Related theoretical derivation, technical discussion and simulation analysis are carried out. From the results, applying the resistive SFCL can effectively limit the transient current rush, guarantee the power balance, and improve the micro-grid system's voltage and frequency stability.

In the near future, a small-scale prototype of the resistive type SFCL will be made, and its application in a real micro-grid system will be tested. The research results will be reported in later articles.

REFERENCES

[1] Mark D. Ainslie, Jumpei Baba, Valerio Salvucci, Tanzo Nitta, Takao Fukunaga, Masatoyo Shibuya, Shinji Torii, Toshiro Matsumura, and Toshiya Kumagai, "Superconducting Fault Current Limiter Design Using Parallel-Connected YBCO Thin Films," *IEEE Trans. Appl. Superconduct.*, vol. 19, no. 3, pp.1918–1921, June 2009.

[2] Steven M. Blair, Campbell D. Booth, Graeme M. Burt, and Chris G. Bright, "Application of Multiple Resistive Superconducting Fault-Current Limiters for Fast Fault Detection in Highly Interconnected Distribution Systems," *IEEE Trans. Power Del.*, vol. 28, no. 2, pp. 1120–1127, Apr. 2013.

[3] Carlos A. Baldan, Jáika S. Lamas, André A. Bernardes, Carlos Y. Shigue, and Ernesto Ruppert, "Fault Current Limiter Using Transformer and Modular Device of YBCO Coated Conductor," *IEEE Trans. Appl. Superconduct.*, vol. 23, no. 3, June 2013, No. 5603804.

[4] Chien-Liang Chen, Virginia Polytech, VA Blacksburg, Yubin Wang, Jih-Sheng Lai, Yuang-Shung Lee, and D. Martin, "Design of Parallel Inverters for Smooth Mode Transfer Microgrid Applications," *IEEE Trans. Power Electron.*, vol. 25, no. 1, pp. 6–15, Jan. 2010.

[5] Jaehong Kim, J.M. Guerrero, P. Rodriguez, R. Teodorescu, and Nam Kwanghee, "Mode Adaptive Droop Control With Virtual Output Impedances for an Inverter-Based Flexible AC Microgrid," *IEEE Trans. Power Electron.*, vol. 26, no. 3, pp. 689–701, Mar. 2011.

[6] M.A. Zamani, A.Yazdani, and T.S. Sidhu, "A Control Strategy for Enhanced Operation of Inverter-Based Microgrids Under Transient Disturbances and Network Faults," *IEEE Trans. Power Del.*, vol. 27, no. 4, pp. 1737–1747, Oct. 2012.

[7] Jong-Fil Moon, and Jin-Seok Kim, "Voltage Sag Analysis in Loop Power Distribution System with SFCL," *IEEE Trans. Appl. Superconduct.*, vol. 23, no. 3, June 2013, No. 5601504.

[8] C.A. Baldan, J.S. Lamas, C.Y. Shigue, and E.R. Filho, "Fault Current Limiter Using YBCO Coated Conductor—The Limiting Factor and Its Recovery Time," *IEEE Trans. Appl. Superconduct.*, vol. 19, no. 3, pp. 1810–1813, June 2009.

[9] Marcelo Gradella Villalva, Jonas Rafael Gazoli, and Ernesto Ruppert Filho, "Comprehensive Approach to Modeling and Simulation of Photovoltaic Arrays," *IEEE Trans. Power Electron.*, vol. 24, no. 5, pp. 1198–1208, May 2009.

[10] Maurizio Cirrincione, Marcello Pucci, and Gianpaolo Vitale, "Neural MPPT of Variable-Pitch Wind Generators With Induction Machines in a Wide Wind Speed Range," *IEEE Trans. Ind. Applicat.*, vol. 49, no. 2, pp. 942–953, Apr. 2013.

[11] Frede Blaabjerg, Remus Teodorescu, Marco Liserre, and Adrian V. Timbus, "Overview of control and grid Synchronization for Distributed Power Generation Systems," *IEEE Trans. Ind. Electron.*, vol. 53, no. 5, pp. 1398–1409, Oct. 2006.

[12] J. A. Peças Lopes, C. L. Moreira, and A. G. Madureira. "Defining Control Strategies for MicroGrids Islanded Operation," *IEEE Trans. Power Syst.*, vol. 21, no. 2, pp. 916–924, May 2006.

[13] S. Elschner, A. Kudymow, S. Fink,W. Goldacker, F. Grilli, C. Schacherer, A. Hobl, J. Bock, and M. Noe, "ENSYSTROB—Resistive fault current limiter based on coated conductors for medium voltage application," *IEEE Trans. Applied Superconduct.*, vol. 21, no. 3, pp. 1209–1212, Jun. 2011.

[14] W. T. B. de Sousa, A. Polasek, F. A. Silva, R. Dias, A. R. Jurelo, and R. de Andrade, Jr., "Simulations and tests of MCP-BSCCO-2212 superconducting fault current limiters," *IEEE Trans. Applied Supercond-uct.*, vol. 22, no. 2, Apr. 2012, No. 5600106.

[15] W. T. B. de Sousa, R. Dias, F. A. da Silva, A. Polasek, and R. de Andrade, Jr., "Comparison Between the Fault Current Limiting Performance of Bi-2212 Bifilar Components and 2G YBCO Coils," *IEEE Trans. Appl. Superconduct.*, vol. 23, no. 3, Jun. 2013, No. 5602204.

[16] L. Ying, J. Sheng, B. Lin, L. Yao, J. Zhang, Z. Jin, Y. Li, and Z. Hong. "AC Loss and Contact Resistance of Resistive Type Fault Current Limiter Using YBCO Coated Conductors," *IEEE Trans. Appl. Superconduct.*, vol. 22, no. 3, June 2012, No. 5602204.

[17] Francesco Grilli and Stephen P. Ashworth, "Quantifying AC Losses in YBCO Coated Conductor Coils," *IEEE Trans. Appl. Superconduct.*, vol. 17, no. 2, pp. 3187–3190, June 2007.

[18] Hyoungku Kang, Jin Bae Na, Yoon Do Chung, and Tae Kuk Ko, "Experimental Study on the Barrier Effects in Gaseous Helium for the Insulation Design of a High Voltage SFCL," *IEEE Trans. Appl. Superconduct.*, vol. 21, no. 3, pp.1328–1331, June 2011.

[19] Jin Bae Na, Hyoungku Kang, and Tae Kuk Ko, "Numerical Analysis and Electrical Insulation Design of a Single-Phase 154 kV Class Non-Inductively Wound Solenoid Type Superconducting Fault Current Limiter," *IEEE Trans. Appl. Superconduct.*, vol. 22, no. 3, June 2012, No. 5602104.